

MALARIA

Activation of mosquito complement antiplasmodial response requires cellular immunity

Julio César Castillo, Ana Beatriz Barletta Ferreira, Nathanie Trisnadi, Carolina Barillas-Mury*

2017 © The Authors, some rights reserved; exclusive licensee American Association for the Advancement of Science.

The mosquito complement-like system is a major defense mechanism that limits *Plasmodium* infection. Ookinete midgut invasion results in irreversible damage to invaded cells and triggers epithelial nitration and complement activation. Several lines of evidence suggest that hemocytes participate in early antiplasmodial responses that target ookinetes, but their role remains unclear. The fate of hemocytes in response to *Plasmodium* infection was investigated by labeling this cell population in vivo. We found that midgut nitration triggers the local release of hemocyte-derived microvesicles (HdMv) into the basal labyrinth of the midgut. Several different strategies, such as gene silencing, immune priming, or systemic injection of polystyrene beads, were used to either enhance or reduce HdMv release. We provide direct experimental evidence that contact of hemocytes with the nitrated midgut basal surface triggers HdMv release and that this response is necessary for effective activation of mosquito complement. Our studies suggest that hemocyte-derived microvesicles may deliver some critical factor(s) that promote activation of thioester-containing protein 1, a key effector of the mosquito antiplasmodial immunity.

INTRODUCTION

Mosquito hemocytes mediate cellular responses to pathogens, such as bacterial phagocytosis (1) and encapsulation of filarial worms (2). They are also involved in the synthesis of key components of the mosquito complement-like system, such as the thioester-containing protein 1 (TEP1) (3). TEP1 is analogous to the vertebrate C3 complement factor and is stabilized in the hemolymph by forming a complex with two leucine-rich proteins, LRIM1 and APL1, that are also synthesized by hemocytes (3–5). *Plasmodium* ookinete invasion causes irreversible damage to midgut epithelial cells (6) and triggers a nitration response that “tags” the parasites for destruction (7). TEP1 binds to the surface of ookinetes that trigger epithelial nitration and forms a complex that ultimately lyses the parasite (8). The mosquito complement-like system is thought to be similar to the vertebrate alternative complement pathway, consisting of a humoral response with sequential activation of a cascade of precursors. A noncatalytic serine protease, SPCLIP1, is an essential convertase cofactor that binds to TEP1 deposited on microbial surfaces and propagates local TEP1 activation (9). Other components of the mosquito complement-like system remain undefined.

Hemocytes are important mediators of immunity that target oocysts (10), but little is known about their role in responses to ookinetes. Exposure of *Anopheles gambiae* mosquitoes to *Plasmodium* infection enhances their ability to respond to subsequent infections (5). This immune priming induces an increase in the number of circulating granulocytes (macrophage-like hemocytes) that is critical to enhance immunity (5). Transcripts of hemocyte-specific genes, such as TEP1 and LRIM1, are transiently detected in midguts dissected at the time when *Plasmodium* ookinetes are invading this organ. Furthermore, transcript levels are greatly increased when challenged mosquitoes are infected a second time (5), suggesting that hemocytes respond to *Plasmodium* invasion by associating with the mosquito midgut. However, it is not clear how hemocytes enhance antiplasmodial immunity. Here, we provide direct experimental evidence that complement activation in *A. gambiae* involves a critical cellular component mediated by hemocyte-derived microvesicles released on the basal surface of nitrated midgut cells undergoing apoptosis in response to ookinete invasion.

RESULTS

We investigated mosquito cellular responses to *Plasmodium* infection by labeling hemocytes in vivo with a hemocyte-specific lipophilic dye (Vybrant CM-DiI) (11), using a modified protocol that allows observation of stained hemocytes for up to 6 days after injection. The fluorescent dye was prominent in two mosquito hemocyte cell types, granulocytes and oenocytoids, circulating in the hemolymph (Fig. 1A) and in sessile granulocytes (Fig. 1, B and C), whereas prohemocytes were weakly stained (fig. S1A). After careful examination of all tissues in adult females, we confirmed that CM-DiI exclusively labels hemocytes (Fig. 1, A to C, and fig. S1B). Hemocyte responses to infection were investigated by feeding dye-injected mosquitoes on *Plasmodium berghei*-infected mice. We were not able to detect intact hemocytes associated with the midgut but instead found fluorescent vesicles associated with *Plasmodium*-invaded epithelial cells undergoing apoptosis (Fig. 1, D to G). One can observe some individual vesicles, but most form plumes of clustered membrane remnants. Vesicles were not observed in noninvaded cells of *Plasmodium*-infected midguts or in midguts from control females fed on healthy mice (Fig. 1E and fig. S1B). Orthogonal sections show ookinetes that have emerged from the basal side of midgut cells and some basal vesicle clusters, as well as vesicles that remained associated with damaged cells as they bud off into the midgut lumen (Fig. 1, F and G, and fig. S2).

Membrane-bound extracellular vesicles can be classified according to their sizes into two main categories: microvesicles (0.1 to 1.0 μm) and exosomes (0.03 to 0.1 μm) (12). The median size of the intact vesicles observed is 0.361 μm (Fig. 1H); thus, we will refer to them as hemocyte-derived microvesicles (HdMv). Besides the colocalization, three additional lines of evidence indicate that the presence of HdMv is associated with ookinete midgut invasion: HdMv are present in 33% of *Plasmodium*-invaded cells but are absent in noninvaded cells from the same midguts (Fig. 1I; $P < 0.0001$, $n = 22$, Mann-Whitney U test), the amount of midgut-associated Vybrant CM-DiI dye (Fig. 1J and table S1) was significantly higher in *P. berghei*-infected midguts than in uninfected sugar-fed ($P < 0.0003$, $n = 7$, t test) or blood-fed controls ($P < 0.0001$, $n = 7$, t test), and the number of HdMv⁺ cells on individual mosquitoes is proportional to the number of ookinetes that invade the midgut (Fig. 1K; $r = 0.8672$, $P < 0.0001$, $n = 22$, linear correlation).

Laboratory of Malaria and Vector Research, National Institute of Allergy and Infectious Diseases, National Institutes of Health, Rockville, MD 20892, USA.

*Corresponding author. Email: cbarillas@niaid.nih.gov

The mosquito priming response to a previous *Plasmodium* infection involves the release of a hemocyte differentiation factor (HDF) that increases the proportion of circulating granulocytes (5). HDF

consists of a complex of lipoxin A4 bound to Evokin, a lipid carrier of the lipocalin family (13). Transfer of cell-free hemolymph with HDF activity also increases granulocytes in the recipient and enhances antiplasmodial immunity (5). We investigated whether this HDF-mediated immune enhancement involved HdMv. The proportion of *Plasmodium*-invaded cells positive for HdMv increased 2.5-fold (from 32.19 to 80.26%) in response to HDF injection (Fig. 2, A and B, and fig. S3; $P < 0.0001$, $n = 26$, Mann-Whitney U test). In addition, the total amount of midgut-associated Vybrant CM-Dil dye (Fig. 2C and table S1) increased by 1.89-fold relative to buffer-injected infected

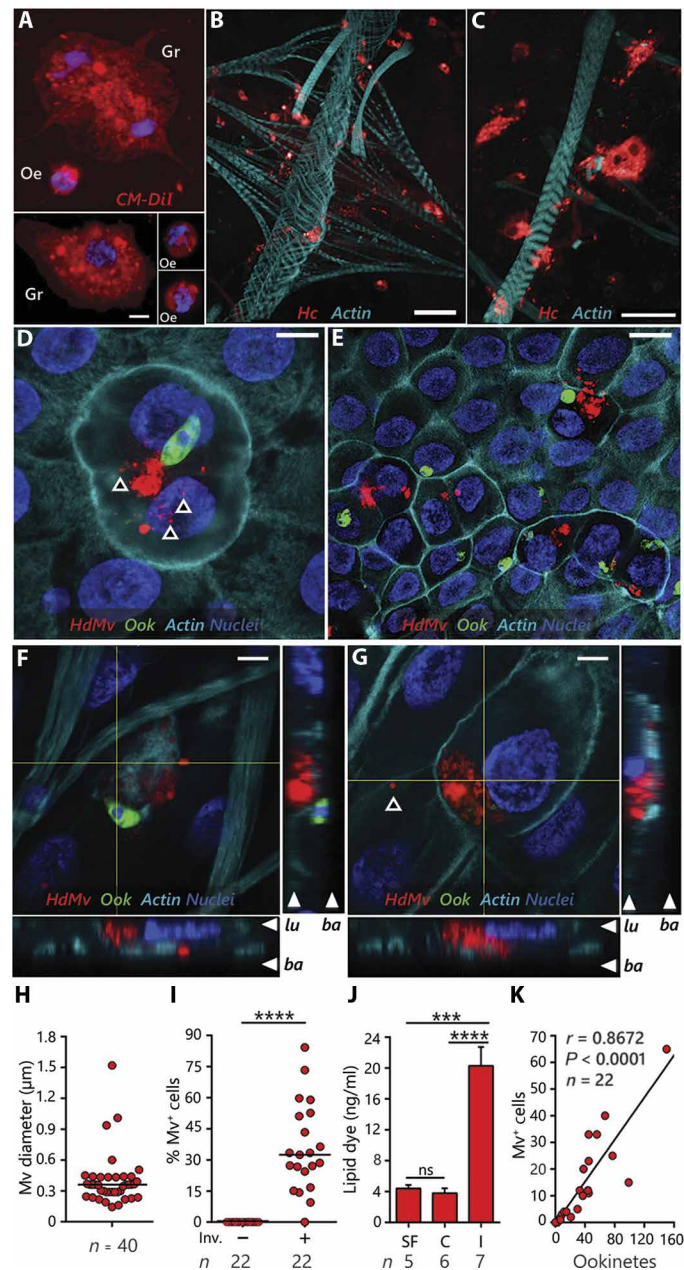


Fig. 1. Mosquito hemocytes' response to *Plasmodium* infection. In vivo hemocyte (Hc) labeling with Vybrant CM-Dil (red). Circulating (A) and sessile hemocytes (B and C). (D to G) Hemocyte-derived microvesicles (HdMv) associated with *Plasmodium*-invaded midgut cells undergoing apoptosis. Actin, cyan; nuclei, blue; parasites, green. Orthogonal sections (F and G) (lu = lumen, ba = basal side, indicated by arrowheads). Gr, granulocytes; Oe, oenocytoids; Ook, ookinets. (H) Size distribution of HdMv. Effect of *P. berghei* infection (I) on the percentage of HdMv⁺ midgut cells and (J) on the amount of CM-Dil associated with sugar-fed (SF), blood-fed control (C), and *P. berghei*-infected midguts (I). ns, not significant. (K) Correlation between the number of HdMv⁺ cells and ookinets on individual midguts (r , Pearson's coefficient). Line indicates medians that were compared using the Mann-Whitney U test, and mean differences in CM-Dil levels were compared using Student's t test (means \pm SEM) (*** $P < 0.001$, **** $P < 0.0001$). Scale bars, 5 μ m (A), 20 μ m (B), and 10 μ m (C to G).

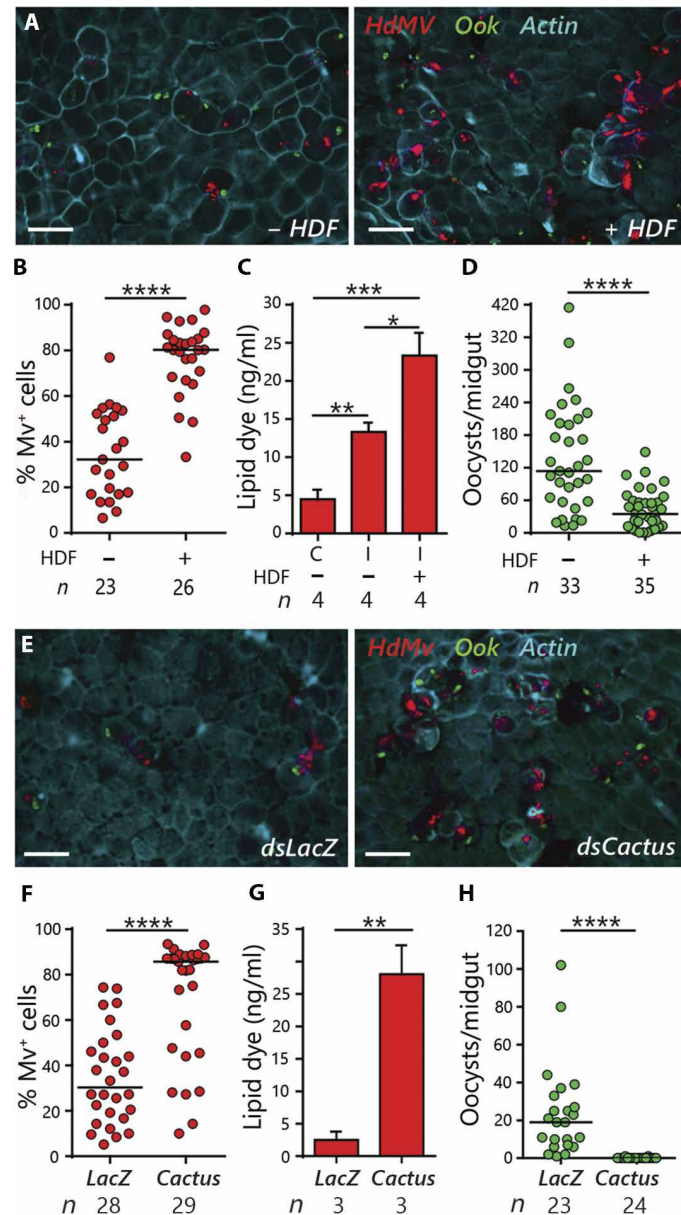


Fig. 2. Effect of enhancing microvesicle release on *Plasmodium* survival. (A to H) Effect of HDF injection (A) or *Cactus* silencing (E) on microvesicle release (B and F), CM-Dil levels (C and G), and *P. berghei* infection (D and H). HdMv, red; actin, cyan; parasites, green. Lines indicate medians that were compared using the Mann-Whitney U test, and mean differences in CM-Dil levels were compared using Student's t test (means \pm SEM) (* $P < 0.05$, ** $P < 0.01$, *** $P < 0.001$, **** $P < 0.0001$). Scale bars, 20 μ m.

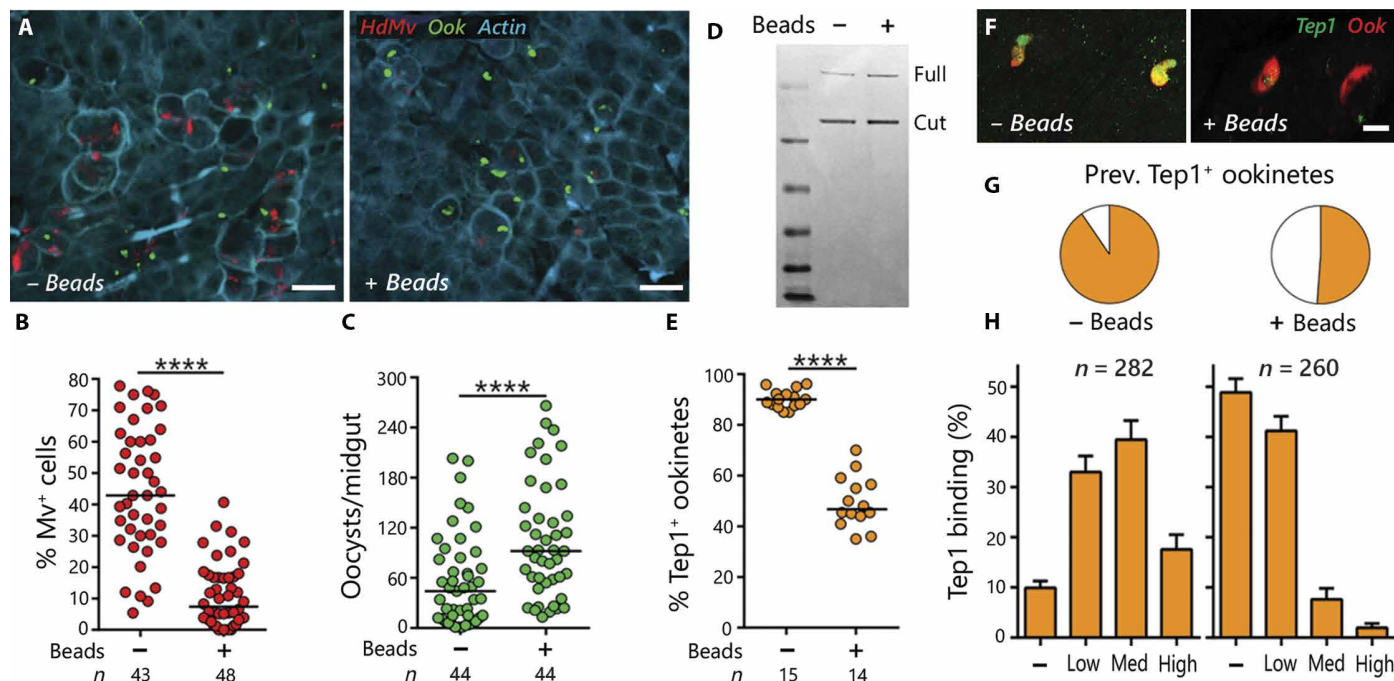


Fig. 3. Effect of hemocyte disruption on microvesicle release and *TEPI* activation in response to *P. berghei* infection. (A and B) Effect of polystyrene bead injection on the percentage of HdMv⁺ midgut cells and (C) *Plasmodium* infection. HdMv, red; actin, cyan; parasites, green. (D) Effect of bead injection on Western blot of *TEPI* protein in cell-free hemolymph (E to H). Effect of bead injection on *TEPI* staining (green) on the ookinete surface (red), on the percentage of *TEPI*⁺ ookinetes in individual midguts (F), on the prevalence of *TEPI*⁺ ookinetes (G), and on the distribution of *TEPI* staining intensity (H). Line indicates medians that were compared using the Mann-Whitney *U* test and frequency distributions were analyzed with χ^2 (*****P* < 0.0001). Scale bars, 20 μ m.

controls ($P = 0.02$, $n = 4$, *t* test) and 5.21-fold relative to uninfected blood-fed controls ($P = 0.001$, $n = 4$, *t* test). HDF injection significantly reduced oocyst numbers (Fig. 2D and fig. S4; $P < 0.0001$, $n = 35$, Mann-Whitney *U* test) and increased the proportion of granulocytes in the recipients (fig. S5; $P = 0.002$, $n = 11$, *t* test).

Overactivation of the *Toll* pathway, by silencing the suppressor *cactus*, greatly enhances *TEPI*-mediated antiplasmodial immunity (14). Furthermore, recent studies revealed that transfer of *cactus*-silenced hemocytes into naïve recipients is sufficient to recapitulate the systemic *cactus*-silencing phenotype, indicating that hemocytes are key mediators of *TEPI*-mediated immunity (15). We investigated whether activation of the *Toll* pathway affects the release of HdMv. *Cactus* silencing increased the proportion of HdMv⁺ invaded cells by 2.83-fold (from 30.3 to 85.71%) (Fig. 2, E and F, and fig. S6; $P < 0.0001$, $n = 29$, Mann-Whitney *U* test) and the amount of midgut-associated Vybrant CM-Dil dye by 11.25-fold (Fig. 2G, fig. S6, and table S1; $P = 0.0054$, $n = 3$, *t* test), relative to the dsLacZ controls. We confirmed that *cactus* silencing markedly enhanced antiplasmodial immunity, rendering mosquitoes highly refractory to infection (Fig. 2H and fig. S7; $P < 0.0001$, $n = 24$, Mann-Whitney *U* test).

Systemic injection of synthetic beads disrupts hemocyte-mediated immune priming in *A. gambiae* mosquitoes (5) and bacterial phagocytosis in *Drosophila* (16). We investigated whether bead injection affects HdMv release and antiplasmodial immunity. We confirmed that injected polystyrene beads are taken up by hemocytes (fig. S8). The number of HdMv in ookinete-invaded cells was greatly reduced in females that were preinjected with polystyrene beads (Fig. 3, A and B, and fig. S9; $P < 0.0001$, $n = 48$, Mann-Whitney *U* test), and the intensity of infection increased significantly (Fig. 3C and fig. S10; $P < 0.0001$, $n = 44$, Mann-Whitney *U* test).

The mechanism by which HdMv affects early immune responses was investigated. Reducing HdMv release by bead injection had no effect on the midgut transcriptional activation of *SRPN6* (a marker of ookinete invasion), *NADPH oxidase 5* (*NOX5*) and *heme peroxidase 2* (*HPX2*) (enzymes that potentiate midgut nitration), or *caspase-S2* and *caspase-S4* (two enzymes induced in cells undergoing apoptosis) (fig. S11). Bead injection also did not affect the levels of the full-length *TEPI* (*TEPI*-full) protein or the proteolytically activated *TEPI* (*TEPI*-cut) protein in the hemolymph (Fig. 3D). However, disruption of HdMv release decreased *TEPI* binding to the ookinete surface (Fig. 3, E to H, and table S2) and reduced the median *TEPI*-positive ookinetes from 90.5 to 51.2% (Fig. 3, E and G, and table S2; $P < 0.0001$, $n = 14$, Mann-Whitney *U* test), as well as the distribution of negative, low, medium, and high *TEPI*-stained ookinetes (Fig. 3H and fig. S12; $P < 0.0001$, $n = 260$ ookinetes, χ^2); therefore, *TEPI* binding was either low or completely absent in 85% of ookinetes from bead-injected mosquitoes (Fig. 3H). *TEPI* staining was not observed on HdMv or in midgut epithelial cells.

We investigated the molecular mechanism that triggers local HdMv release. It is well established that disrupting midgut nitration prevents *TEPI* activation and enhances parasite survival (8). However, the mechanism remained unclear. We explored the hypothesis that contact with a nitrated midgut basal lamina is the signal that triggers loss of integrity of hemocytes and local microvesicle release. Disruption of epithelial nitration by silencing *NOX5* and *HPX2*, two enzymes that potentiate nitration (8), reduced HdMv release in response to ookinete invasion by 7.5-fold (Fig. 4A and figs. S13 and S14; $P < 0.0001$, $n = 19$, Mann-Whitney *U* test). Silencing *IMPer*, a peroxidase that limits the permeability of immune elicitors released by

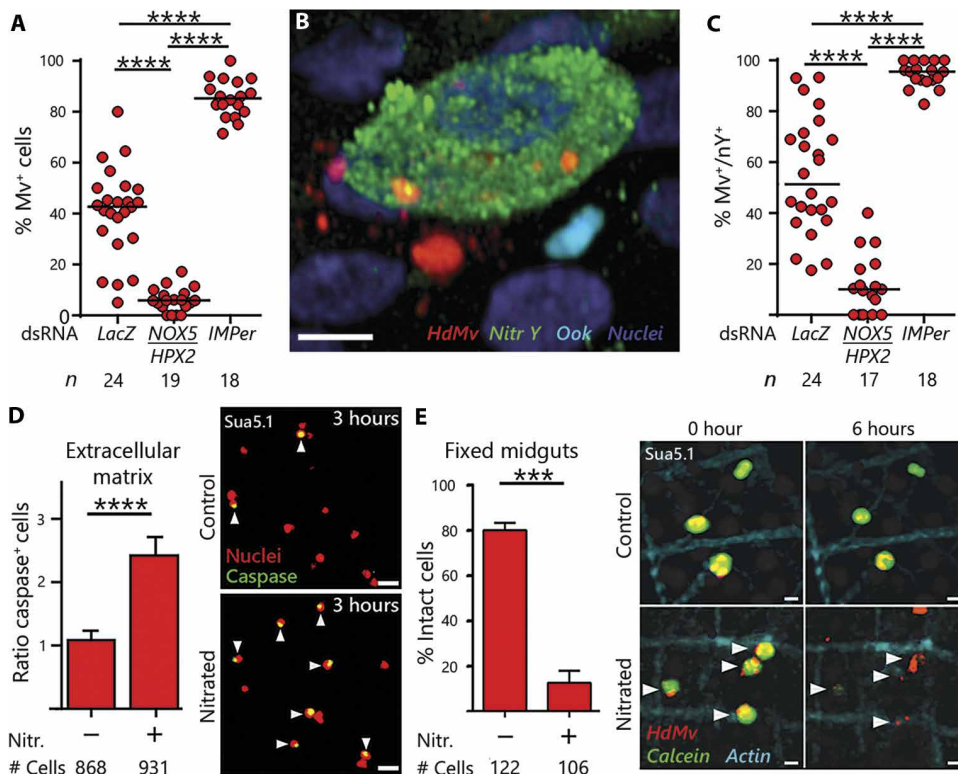


Fig. 4. Effect of nitration on microvesicle release. (A to C) Effect of reducing nitration by silencing *NOX5/HPX2* or enhancing it by silencing *IMPer* on the proportion of invaded *HdMv*⁺ cells (A) and on the proportion of nitrated *HdMv*⁺ cells (C). Association of *HdMv* with nitrated cells undergoing apoptosis (B). *HdMv*, red; nitrotyrosine, green; ookinete, cyan; nuclei, blue. Medians are indicated by the black line and compared using the Mann-Whitney *U* test. (D) Effect of contact of *Sua5.1* cells with a nitrated extracellular matrix on the rate of apoptosis, nuclei (red), and nuclei of caspase⁺ apoptotic cells (green; see arrowheads). (E) Effect of contact with nitrated midguts on cell integrity measured by retention of cytoplasmic calcein (green), *HdMv* (red), and actin (cyan). Line indicates medians that were compared using the Mann-Whitney *U* test (****P* < 0.001, *****P* < 0.0001). Scale bars, 10 μ m.

Plasmodium in the midgut lumen (17), enhances nitration and greatly reduces parasite survival (8). *IMPer* silencing increased the proportion of *HdMv*⁺ invaded cells by 2.13-fold (from 45 to 96%) (Fig. 4A, figs. S13 and S14, and table S3; *P* < 0.0001, *n* = 18, Mann-Whitney *U* test). *HdMv* were often associated with nitrated midgut cells (Fig. 4B). Furthermore, the proportion of *HdMv*⁺ cells that were nitrated was greatly reduced when *NOX5* and *HPX2* were silenced (Fig. 4C, fig. S15, and table S3; *P* < 0.0001, *n* = 17, Mann-Whitney *U* test), whereas *IMPer* silencing had the opposite effect and enhanced the association (Fig. 4C, fig. S14, and table S3; *P* < 0.0001, *n* = 18, Mann-Whitney *U* test).

Last, we tested whether contact with a nitrated surface was sufficient for hemocytes to lose their integrity and release vesicles using *in vitro* assays. *Sua5.1* hemocyte-like phagocytic *A. gambiae* cultured cells (18) were labeled with the same fluorescent dye and allowed to come in contact with either a nitrated extracellular matrix or fixed nitrated midguts. Contact with a nitrated extracellular matrix for 3 hours enhanced apoptosis by 2.5-fold relative to cells in contact with a matrix that was not nitrated (Fig. 4D and table S4; *P* < 0.0001, *n* = 931 cells, *t* test), whereas contact with the basal surface of fixed nitrated midguts increased the loss of cellular integrity and vesicle release after 6 hours by eightfold, relative to those in contact with fixed non-nitrated midguts (Fig. 4E, fig. S15, table S5, and movies S1 to S4; *P* < 0.0001, *n* = 106 cells, *t* test). Cells in chambers with either nitrated or non-nitrated

midguts that did not come in direct contact with the midgut surface maintained their integrity (fig. S17 and movie S5).

DISCUSSION

Our findings indicate that hemocytes detect injury caused by ookinete invasion and come in close contact with the basal surface of the midgut (Fig. 5). Contact with a nitrated midgut basal lamina is sufficient to trigger apoptosis and vesicle release. *HdMv* promote TEP1 binding to the ookinete surface and are necessary to mount an effective antiplasmodial response. However, the precise mechanism by which *HdMv* promote complement activation remains to be defined.

In the 12 years since the initial report on the role of TEP1 in antiplasmodial activity (3), there has been limited progress in the biochemical identification of other components of the mosquito complement system, and efforts to establish an *in vitro* system to activate this cascade have not been successful. The fact that local release of *HdMv* is required to activate mosquito complement suggests that *HdMv* may deliver a high local concentration of some critical factors [for example, a convertase and/or a convertase cofactor (such as SPCLIP1) (9)] that are required for activation and deposition of TEP1 on the ookinete surface (Fig. 5). The *Sua5.1* cell line also responds to contact with nitrated midgut surfaces by releasing microvesicles and opens the possibility of isolating intact microvesicles and identifying the factor(s) they carry.

Another remaining question is the identity of the hemocyte population releasing the microvesicles. Unfortunately, the classification of mosquito hemocyte types is based on morphology, and we only observed cell remnants associated with invaded midgut cells. However, three lines of evidence suggest that granulocytes are releasing *HdMv*: (i) Priming greatly increases the proportion of circulating granulocytes and also enhances *HdMv* release. (ii) Melanization reactions were never observed in *Plasmodium*-infected midguts (in *A. gambiae* G3 females), a response one would expect if oenocytoids were involved, because this cell type expresses high levels of phenoloxidase activity. (iii) Granulocytes have strong phagocytic capacity and readily take polystyrene beads, and we know that this treatment greatly reduces *HdMv* release. In summary, granulocytes appear to be the major players, but one cannot rule out that other cell types may also participate. Cell-specific markers would be required to address this important question, but they are not yet available.

These findings provide a point of convergence to understand the complex interactions between epithelial and cellular immunity, complement activation and innate immune memory in mosquitoes, and how they determine malaria transmission. The discovery that nitration of the extracellular matrix can trigger complement activation

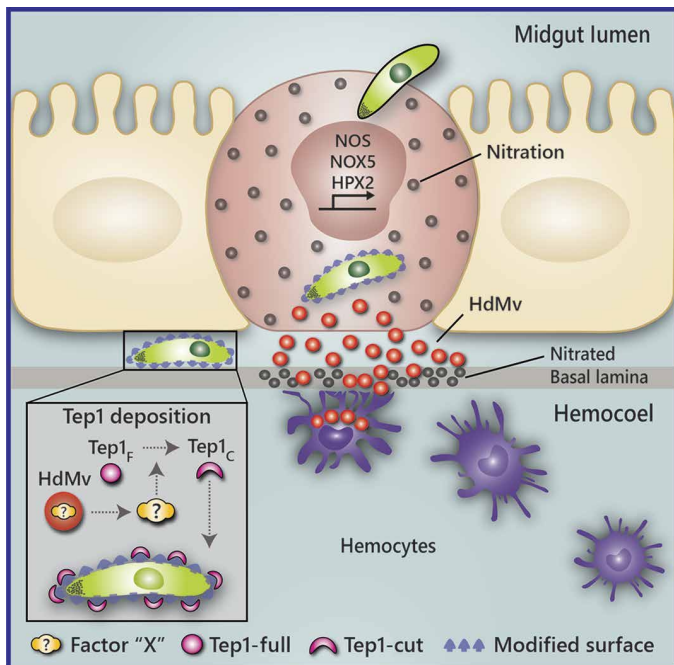


Fig. 5. Proposed model of the role of HdMv on mosquito complement activation. Ookinete invasion causes irreversible cell damage; activates a nitration response that involves the induction of nitric oxide synthase (NOS), NOX5, and HPX2; and attracts hemocytes to the basal surface of the midgut. Contact of hemocytes with the nitrated surface of the basal lamina triggers the release of HdMv. Activation of circulating full-length TEP1 (TEP1-full) requires a proteolytic cleavage to generate TEP1-cut that deposits on the parasite's surface (3, 25). Because HdMv release is necessary to activate the mosquito complement system, we propose that HdMv may contain a factor or factors (such as a convertase and/or a convertase cofactor) that promote TEP-1 activation.

through a mechanism that involves cellular immunity may also have broad implications in humans. Nitration is often used as a biomarker of tissue damage, but our studies suggest that it may also be a signal that promotes local complement activation through a microvesicle-mediated mechanism. We conclude that, besides the humoral factors present in the hemolymph, activation of the mosquito complement-like system also requires a cellular response involving local microvesicle release. Our findings suggest that, under some conditions, activation of the alternative pathway of complement in vertebrates may also involve a similar ancestral cellular innate immune response.

MATERIALS AND METHODS

Study design

Research objectives.

This study aimed to examine the role of hemocytes in mosquito antiplasmodial responses that target early stages of *Plasmodium* infection in the mosquito midgut.

Research samples.

Tissue samples (midguts, hemocytes, hemolymph, or whole body) were collected from adult mosquito females 1 to 6 days after emergence depending on the experimental setup, as indicated on each section. SuA5.1 cells were cultured in vitro and seeded at similar confluency in all experiments.

Experimental design.

To evaluate the effect of infection on a given parameter, we fed experimental and control groups of adult female mosquitoes on either a *P. berghei*-infected or a control (healthy) mouse. The effect of a given treatment on infection was evaluated by feeding the control (untreated mosquitoes) and experimental groups on the same mouse, by simultaneously placing the anterior end of the mouse on one mosquito cup and the posterior on the second cup. Mice were rotated head-to-tail every 7 to 10 min to ensure uniform feedings. Tissues were dissected and fixed, and the prevalence of HdMv⁺ cells in different experimental settings was quantitated from confocal images or by direct counting. The amount of hemocyte-derived lipids associated with the midgut was established by measuring the concentration of CM-DiI dye in midgut tissues after lipid extraction. TEP1 binding to the ookinete surface was determined by immunofluorescence staining. *P. berghei* infections were evaluated day 10 after infection. For in vitro assays using Sua5.1 cells, cells were cocultured with extracellular matrix or midguts that were either nitrated or not.

Randomization.

In all experiments, mosquitoes from the control and experimental groups came from the same cohorts/generation, were reared under the same environmental conditions, and were age-matched. Adult mosquito females were randomly placed in either the control group or the experimental group.

Sample size.

The number of mosquitoes analyzed for each different experimental approach is indicated on each figure. In a typical in vivo experiment, groups of 30 to 50 mosquitoes were used for each control or experimental group, and for in vitro experiments with Sua5.1 hemocyte-like cells, 1.5×10^5 cells were used.

Ethics statement

Public Health Service Animal Welfare Assurance #A4149-01 guidelines were followed according to the National Institutes of Health (NIH) Office of Animal Care and Use. These studies were carried out according to the NIH animal study protocol (ASP) approved by the NIH Animal Care and User Committee, with approval ID ASP-LMVR5.

Mosquito rearing and *P. berghei* infection

A. gambiae mosquitoes (G3 strain) were reared on a 12-hour light/dark cycle at 27°C and 80% humidity and fed ad libitum with 10% dark Karo syrup solution. *P. berghei*-green fluorescent protein (GFP) parasites (GFP-CON transgenic 259cl2 strain) (19) were maintained by serial passage in 4- to 5-week-old female BALB/c mice, and parasitemia was determined by counting the numbers of parasites from methanol-fixed blood smears stained with 10% Giemsa. Mosquito infections were carried out by allowing female mosquitoes to feed on gametocytemic mice (3.5 to 4.5% parasitemia, 1 to 2 exflagellations) 2 to 3 days after blood passage from infected donors (20). To determine infection levels, we counted *Plasmodium* oocysts from dissected midguts 7 to 10 days after infection. Midguts were dissected in 1× phosphate-buffered saline (PBS), fixed in 4% paraformaldehyde for 20 min, washed, mounted, and counted using a fluorescent microscope equipped with a GFP filter.

Antibiotic treatment

To generate microbiota-free mosquitoes, newly enclosed females were given water containing penicillin (100 U/ml)-streptomycin (0.1 mg/ml) (Sigma-Aldrich) 2 days before blood feeding and for 3 days after feeding. Sugar was provided as a dry sugar cube.

Hemolymph collection and cell counting

Hemolymph was collected using a previously developed procedure (21), with some added modifications. Briefly, an incision was made in the abdominal wall between the last two abdominal segments using a sterile scalpel, and 10 μ l of perfusion buffer [60% Schneider's medium, 10% fetal bovine serum (FBS), and 30% citrate buffer (pH 4.5; 98 mM NaOH, 186 mM NaCl, 1.7 mM EDTA, and 41 mM citric acid)] was gradually injected into the thorax; a total of 10 μ l of diluted hemolymph was collected from the incision using a siliconized pipette tip. Hemolymph samples were immediately placed in a sterile disposable hemocytometer slide (Neubauer Improved, iNCYTO C-Chip DHC-N01, www.incyto.com). To count granulocytes, we counted the total number of hemocytes in five quadrants using a compound microscope at 40 \times , and the number of granulocytes was determined as a fraction on the total number present on each sample. For each experiment, groups of 10 to 12 mosquitoes were counted, and the number of cells was expressed as means \pm SEM.

Production of HDF

To generate primed mosquitoes, we challenged 4-day-old female mosquitoes with *P. berghei*-GFP. Challenged females were kept at 21°C for 48 hours to allow *P. berghei* infection and midgut invasion, at the end of which they were transferred to 28°C to reduce the level of infection. HDF-containing hemolymph was collected from challenged (primed) donors 7 days after priming using a modified anticoagulant buffer containing 95% Schneider's medium and 5% citrate buffer. Cell-free supernatant was collected after centrifugation at 4°C at 9300g for 10 min, aliquoted, and stored at -80°C until needed. HDF-containing cell-free hemolymph was transferred from donor mosquitoes into recipient animals, as previously described (9), by injecting 2-day-old females with 138 nl of diluted HDF (1:10) using a Drummond Nanoject. To determine HDF bioactivity, we measured oocyst development 7 days after infection and granulocyte differentiation 5 days after injection (figs. S6 and S7).

Hemocyte labeling and CM-Dil injection

In vivo hemocyte staining was achieved using the hemocyte specific dye Vybrant CM-Dil (Life Technologies), as described earlier (11), with some modifications. Briefly, female mosquitoes were injected with 138 nl of a labeling solution containing 140 μ M Vybrant CM-Dil, prepared freshly in sterile water, using a microcapillary glass needle and a Drummond Nanoject. Shortly after CM-Dil injection, mosquitoes were allowed to recover at 27°C until needed. To assess hemocyte labeling, labeled hemocytes were collected as early as 24 hours after injection by perfusion and allowed to adhere to a poly-L-lysine-coated glass slide at room temperature for 30 min, fixed for 10 min in 4% paraformaldehyde in 1 \times PBS, washed three times in PBS for 5 min, counterstained with 4',6-diamidino-2-phenylindole (DAPI) (10 μ g/ml; Life Technologies) and phalloidin (0.165 μ M; Life Technologies), and mounted on a drop of Vectashield (Vector Laboratories) for observation using a fluorescent microscope. To assess tissue labeling background, midguts, ovaries, and abdomens of DiI-injected females were dissected 24 hours after injection, fixed in 4% paraformaldehyde, rinsed five times in 1 \times PBS, counterstained with DAPI and Alexa Fluor 633 phalloidin, and mounted in Vectashield (Vector Laboratories).

Lipid (CM-Dil) quantification

Midgut-associated CM-Dil (HdMv) was extracted using a slightly modified lipid extraction protocol developed by Bligh and Dyer (22).

Briefly, 10 dissected midguts from DiI-injected mosquitoes were macerated in 100 μ l of transfer buffer (95% Schneider's medium and 5% citrate buffer) using a plastic pestle. Homogenates (100 μ l) were then mixed with chloroform and methanol in a 0.8:1.0:2.0 ratio (v/v/v) in a 1.5-ml Eppendorf tube, thoroughly vortexed every 10 min for 1 hour, and then centrifuged at 580g for 10 min at room temperature. The supernatant was transferred to a new glass tube and mixed with an additional 62.5 μ l of Milli-Q water and 62.5 μ l of chloroform, vigorously vortexed, and then centrifuged at 580g for 10 min to induce phase separation. The organic phase was carefully transferred to a clean 1.0-ml glass tube (8 \times 40 mm, clear SepCap vial, Thermo Fisher Scientific) and dried with nitrogen gas. Dried samples were then resuspended in 20 μ l of isopropanol and kept on ice, and absorbance values were measured at 573 nm on a Nanodrop fluorometer (Thermo Fisher Scientific). To calculate the concentration of DiI/midgut, we plotted a standard curve (10 to 100 ng/ml) and the calculated linear equation $y = 1.407x - 4.088$.

Midgut immunostaining

Mosquito midgut immunostainings were performed as previously described (4). Briefly, mosquitoes were injected with CM-Dil 48 hours before blood feeding and subsequently fed on an infected mouse (3 to 4.5% parasitemia) and incubated at 21°C. Twenty-four hours after blood feeding, midguts were dissected in 1 \times PBS, fixed for 40 s in 4% paraformaldehyde, and opened longitudinally in PBS (pH 7.2) to gently remove the blood bolus. Cleaned midguts were then fixed in freshly prepared 4% paraformaldehyde in 1 \times PBS for 1 hour at room temperature, permeabilized, and blocked in PBT [PBS supplemented with 1% bovine serum albumin (BSA) and 0.1% Triton X-100] for 1 to 2 hours at room temperature. Midguts were then incubated overnight with mouse α -Pbs21 (1:300 in PBT) primary antibody at 4°C and washed three times (10 min each) with PBT, followed by a 2-hour incubation at room temperature with the secondary antibody (Alexa Fluor 488-conjugated antibody diluted 1:500 in PBT) at room temperature. Last, immunostained tissues were washed three times in PBT, counterstained with Alexa Fluor 633 phalloidin (actin, 0.165 μ M) and DAPI (nuclei, 10 μ g/ml), and lastly mounted in Vectashield (Vector Laboratories). Immunostaining preparations were analyzed by fluorescence and confocal microscopy. To estimate the number of *HdMv*⁺ midgut cells (DiI⁺ cells), we counted the total number of DiI-containing invaded cells and the total number of ookinetes per midgut. Invaded cells were defined as cells that contained an intact ookinete either inside or within three cell diameters away and displayed the typical "bulging out" phenotype described (7).

Double-stranded RNA synthesis and gene silencing

Double-stranded RNA (dsRNA) for *Cactus*, *IMPer*, *NOX5*, and *HPX2* were synthesized by in vitro transcription using the MEGAscript RNAi Kit (Ambion). DNA templates were obtained by polymerase chain reaction (PCR) using *A. gambiae* complementary DNA (cDNA) extracted from *Plasmodium*-infected midguts dissected 24 hours after blood feeding and primer pairs containing T7 polymerase promoter sites added to the 5'-end (table S6). dsRNA for *LacZ* was synthesized from a DNA template amplified from a cloned fragment, as previously described (8). Briefly, mosquitoes were injected with 138 nl of CM-Dil (140 μ M) on day 1 after emergence and with 69 nl of a dsRNA solution (3 μ g/ μ l) (207 ng of dsRNA) on day 2 and blood-fed on a *Plasmodium*-infected mouse 3 days later (day 5). For *NOX5*/*HPX2*

double silencing, mosquitoes were injected with two shots (1:1 equimolar mix of both dsRNA stock solutions). For IMPer silencing, mosquitoes were injected with dsRNA 28 hours before blood feeding.

Microinjection of beads

Two-day-old females were injected in the thorax (dorsally) with CM-DiI, as described above, and allowed to recover for 48 hours. After CM-DiI injection, female mosquitoes were blood-fed (day 4) on an infected mouse (3.5 to 4.5% parasitemia) and allowed to recover for 6 to 8 hours at 21°C after blood feeding to allow parasites to undergo fertilization. After fertilization, mosquitoes were subsequently injected with 1.0 μM polystyrene beads (FluoSpheres, Life Technologies) on the opposite dorsal side of the thorax. Injections were performed as follows: Mosquitoes were quickly cold-anesthetized in groups of 10 and injected with 138 nl of HBSS buffer (Hanks' basal salt solution, Life Technologies) per mosquito or $\sim 200,000$ beads per mosquito diluted in HBSS buffer. After injection, mosquitoes were quickly transferred to 21°C to resume normal parasite development. To assess the effect of bead injection on the production of *HdMvs*, we counted the number of Mv^+ cells from the total number of invasion events per midgut by visual inspection of immunolabeled midguts from buffer- or bead-injected mosquitoes dissected 24 hours after infection. After dissection, midguts were fixed and processed for immunostaining using the primary antibody α -*Pbs21* (1:300) and Alexa Fluor 488-conjugated secondary antibody (1:500) (Life Technologies), DAPI (nuclei), and Alexa Fluor 633 phalloidin (actin), and mounted in Vectashield. To examine the effect of bead injection on *P. berghei* infection, we treated mosquitoes as indicated above, and oocysts were allowed to develop and counted 10 days after infection. Pearson's *r* value ($\alpha = 0.05$) was calculated for correlation analysis between the number of Mv^+ midgut cells and the number of ookinetes per midgut. Proportion differences were analyzed using the Mann-Whitney *U* test and expressed as means \pm SEM.

RNA isolation and gene expression analysis

For gene expression analysis, midguts were dissected 24 hours after blood meal (18 hours after bead/buffer injection) in 1 \times sterile PBS and collected directly in 300 μl of Buffer RLT (Qiagen) supplemented with β -mercaptoethanol, homogenized for 1 min using a sterile plastic pestle, and flash-frozen in liquid nitrogen. Total RNA was extracted using the RNeasy RNA extraction kit (Qiagen) according to the manufacturer's instructions, and the quality of each RNA sample was measured on a NanoDrop (Thermo Fisher Scientific). cDNA was prepared using 1 μg of RNA per sample as template using the QuantiTect reverse transcription kit and DNA wipeout (Qiagen). The resulting cDNA was then used as template for relative quantitation by quantitative PCR (qPCR) using the SYBR green DyNAmo HS qPCR mix (Thermo Fisher Scientific) and gene-specific primers listed in table S6. Expression levels were normalized using the *rpS7* gene (ribosomal protein S7) relative to uninfected blood-fed controls. Real-time PCRs were performed on a CFX96 Real-Time PCR detection system (Bio-Rad), and data were analyzed postrun using the $2^{-\Delta\Delta C_t}$ method (23). Samples were run under standard conditions using 0.5 μM of each primer and the following cycle conditions: initial denaturation at 95°C for 15 min and 40 cycles of amplification (denaturation at 94°C for 10 s, annealing at 55°C for 20 s, and extension at 72°C for 30 s), followed by a final extension at 72°C for 10 min. For each experiment, we measured gene expression of at least two biological replicates per experiment, with each biological sample consisting of 20 midguts. All reactions were run

in duplicates, and the gene expression differences reported were based on three independent experiments and analyzed using the Student's *t* test.

TEP1 protein detection by Western blot

TEP1 protein levels were measured by Western blot, as previously described (24). Hemolymph from seven mosquitoes (5 μl per mosquito) preinjected with buffer or beads, as described, was collected 24 hours after infection by perfusion using ice-cold transfer buffer (95% Schneider's medium and 5% citrate buffer). Hemolymph was collected using siliconized tips into a siliconized tube containing 10.5 μl of NuPAGE LDS Sample Buffer, 3 μl of protease inhibitor (cComplete EDTA-free protease inhibitor cocktail; Roche), and 1.5 μl of β -mercaptoethanol. Protein samples (40 μl) were separated in a 4 to 12% bis-tris NuPAGE gel (Novex, Life Technologies) in 1 \times Mops for 45 min. After electrophoresis, proteins were transferred to a nitrocellulose membrane using the iBlot transfer system (Life Technologies) under semidry conditions and blocked with 5% nonfat milk in TBT [0.05 M tris, 0.138 M NaCl, 0.0027 M KCl (pH 8), and 0.1% Tween 20] for 2 hours at room temperature, followed by overnight incubation at 4°C with rabbit α -*TEP1* (1:1000, provided by M. Povelones, University of Pennsylvania) diluted in blocking buffer. Subsequently, the membrane was washed three times in TBT for 10 min each and incubated for 4 hours at room temperature with anti-rabbit IgG-alkaline phosphatase conjugate diluted 1:4000 in blocking buffer. Protein bands were detected using Western Blue stabilized substrate (Promega) for 15 min.

Detection of TEP1 protein binding in ookinetes by immunofluorescence

Four-day-old female mosquitoes were blood-fed on an infected mouse (3.5 to 4.5% parasitemia) and injected with beads or buffer, as previously described. Infected midguts were dissected 24 hours after infection, cleaned, fixed, blocked using PBT [1 \times PBS (pH 7.4), 1% BSA, and 0.1% Triton X-100] for 1 hour, and double-stained overnight using mouse α -*Pbs21* (1:300) and rabbit α -*TEP1* (1:500) (provided by M. Povelones). Midguts were then washed three times in PBT supplemented with 0.1% gelatin (PBT-Gelatin) and incubated with the secondary antibodies donkey α -rabbit (Alexa Fluor 488) and goat α -mouse (Alexa Fluor 633). Last, midguts were washed four times with PBT-Gelatin and counterstained with DAPI (nuclei) and phalloidin (actin). *TEP1*-positive or *TEP1*-negative parasites were counted from a total of 20 midguts (two experiments, 10 midguts each). To quantify the percentage of positive parasites that were *TEP1*_{Low}, *TEP1*_{Medium}, or *TEP1*_{High}, we counted about 15 to 30 parasites per randomly selected midgut (total of 10 midguts) from two separate experiments.

Immunodetection of epithelial nitration

Newly emerged mosquitoes were injected with CM-DiI, as previously described, followed by injection of dsRNA of NOX5, HPX2, and LacZ and allowed to recover for 3 days before blood feeding. IMPer-silenced mosquitoes were injected with dsRNA 1 day before blood feeding. Silenced mosquitoes were blood-fed on an infected mouse (3.5 to 4.5% parasitemia) and dissected 28 to 30 hours after infection, cleaned, fixed, blocked using PBT [1 \times PBS (pH 7.4), 1% BSA, and 0.1% Triton X-100] for 1 hour, and double-stained overnight using rabbit α -GFP (1:2000) (Abcam, rabbit anti-GFP, Ab290) and mouse α -nitrotyrosine (1:150) (Cayman Chemical, item # 189542). Midguts were then washed three times in PBT-Gelatin and incubated with the secondary antibodies

donkey α -rabbit (Alexa Fluor 488) and goat α -mouse (Alexa Fluor 633). Last, midguts were washed four times in PBT-Gelatin and counterstained with DAPI (nuclei) and phalloidin (actin). The percentages of DiI⁺ invaded cells and of DiI⁺ cells that were also positive for nitrotyrosine⁺ (nY⁺) were calculated based on absolute counts per individual midgut. Proportion differences were analyzed using the Mann-Whitney *U* test and expressed as means \pm SEM.

Insect cell culture

The Sua5.1 hemocyte-like cell line was maintained at 28°C in an incubator without CO₂ injection using Schneider's medium supplemented with 10% FBS and penicillin (100 U/ml) and streptomycin (100 μ g/ml).

Preparation of an artificial extracellular matrix

A solid acellular extracellular matrix was developed using collagen I (1.5 mg/ml; Advanced Biomatrix), fibronectin (2.5 μ g/ml; Sigma-Aldrich), 200 μ g of purified BSA (Sigma-Aldrich), and RPMI 1640 neutralized with Hepes. After mixing all the components, matrix pH was neutralized with 0.3 mM NaOH, placed in an eight-well chamber (Ibidi μ -Slide 8-well), and allowed to polymerize at 37°C for 30 min.

Live caspase activity assays

After polymerization, the collagen matrix was subjected to an in vitro nitration reaction using 50 mM sodium phosphate buffer, 1 mM H₂O₂ (hydrogen peroxide), 1 mM sodium nitrite (NaNO₂), and HRP (horseradish peroxidase) (1 U/ml). The reaction was carried out at 37°C for 30 min. After the reaction, the matrix was washed at least three times with Schneider's medium supplemented with 10% FBS to wash off unreacted components. Control matrix was incubated with all reaction components except for sodium nitrite. Live Sua5.1 hemocyte-like cells (1.5×10^5 cells) were labeled with 20 μ M Hoechst 33342 (Thermo Fisher Scientific) and then seeded in the solid collagen matrix for both control and nitrated conditions in the presence of 2.5 μ M CellEvent Caspase-3/7 Green Detection Reagent (Thermo Fisher Scientific). Five fields from each condition were imaged at 30 min and 3 hours. The 30-min time point served as a baseline for caspase fluorescent signal. Four independent replicates were completed, and a minimum of 600 cells at 30 min and 800 cells at 3 hours were counted. Images were analyzed using Imaris 8.3.1 spot detection with identical threshold settings. Caspase signal baseline was subtracted from data collected at the 3-hour time point. Caspase activity fold change was calculated using the control 3 hours after seeding as a reference.

Live cell membrane integrity assays

Four-day-old mosquitoes were fed with a saline solution (150 mM NaCl and 10 mM NaHCO₃) kept at 37°C using a standard membrane feeder. One hour after feeding, midguts were dissected in 4% paraformaldehyde in PBS (pH 7.4) and quickly fixed for 30 to 40 s to maintain the tissue in a distended state. Tissues were then emptied by creating a small incision in the posterior midgut to drain contents. Tissues were then fixed for 1 hour at room temperature with 4% paraformaldehyde in PBS. After fixation, midguts were washed with PBS containing 1% BSA. Similar to matrix nitration, midgut nitration reactions were performed using 50 mM sodium phosphate buffer, 1 mM H₂O₂, 1 mM sodium nitrite, and HRP (1 U/ml). The reaction was carried out at 37°C for 30 min. The control reaction contained all the components previously described except for sodium nitrite. Midguts were washed with PBS containing 1% BSA and stained with 1 U of phal-

loidin (Alexa Fluor 633, Molecular Probes) and 20 μ M Hoechst for 30 min at room temperature. After staining, midguts were embedded in a solid collagen matrix, as previously described. Sua5.1 cells were incubated with 5 μ M Vybrant CM-DiI in Schneider's medium without serum for 1 hour at room temperature and then washed three times with Schneider's medium. The next day, cells were dissociated, and about 1.5×10^5 cells were stained with 2 μ M calcein AM (Thermo Fisher Scientific) and then seeded with medium containing 2 μ M calcein AM over the solid collagen matrix containing embedded midguts. Imaging began 30 min after seeding to allow cells to settle on top of the midgut and the matrix. A *z*-stack encompassing cells and the midgut was taken every 10 min for a total of 6 hours. Scan time varied between 1 and 1.5 min depending on *z*-stack thickness. All conditions were imaged using identical parameters with 5% or less laser power for all wavelengths. Images were analyzed using Imaris 8.3.1 spot detection with identical threshold settings. Cells that moved out of frame or moved between the midgut and the matrix were not included in the analysis.

Confocal imaging

Images were collected using a Leica TCS SP5 confocal microscope (Leica Microsystems) using a 40 \times , 63 \times , or 100 \times oil immersion objective (numerical aperture, 1.25 to 1.4) and equipped with photomultiplier tube/hybrid detectors. Fluorochromes were excited using a 488-nm argon laser for Alexa Fluor 488/GFP/caspase, a DPSS 561-nm laser for CM-DiI, and a HeNe 633-nm laser for Alexa Fluor 633. DAPI and Hoechst were excited using a 405-nm diode laser. Images were taken using sequential acquisition and variable *z*-steps. Images were processed using ImageJ (1.50i), Leica LAS AF software (version 3.2), Imaris 7.7.1 or 8.3.1 (Bitplane AG), and Adobe Photoshop CC (Adobe Systems).

Statistical analysis

All statistical analyses were performed using Prism 7.01 for Windows (GraphPad Software Inc.). All pairwise comparisons were analyzed using the unpaired Student's *t* test (parametric) or the Mann-Whitney *U* test (nonparametric). Frequency distributions were analyzed using χ^2 , and Pearson's *r* value ($\alpha = 0.05$) were calculated for correlation analysis. Significance was assessed at $P < 0.05$, and error bars represent the SEM.

SUPPLEMENTARY MATERIALS

immunology.sciencemag.org/cgi/content/full/2/7/eaal1505/DC1

Fig. S1. Confocal imaging of mosquito organs after systemic injection of the lipophilic dye Vybrant CM-DiI.

Fig. S2. Confocal staining of midguts of mosquitoes injected with Vybrant CM-DiI, 24 hours after feeding on a *P. berghei*-infected mouse.

Fig. S3. Effect of HDF injection on the percentage of ookinete-invaded cells positive for hemocyte-derived microvesicles (HdMv⁺).

Fig. S4. Effect of HDF injection on *P. berghei* infection.

Fig. S5. Effect of HDF injection on proportion of granulocytes.

Fig. S6. Effect of *Cactus* silencing on the percentage of ookinete-invaded cells positive for hemocyte-derived microvesicles (HdMv⁺).

Fig. S7. Effect of *Cactus* silencing on *P. berghei* infection.

Fig. S8. Confocal image of polystyrene beads inside a phagocytic granulocyte 24 hours after systemic bead injection.

Fig. S9. Effect of hemocyte disruption by systemic injection of polystyrene beads on the percentage of ookinete-invaded cells positive for hemocyte-derived microvesicles (HdMv⁺).

Fig. S10. Effect of hemocyte disruption by bead polystyrene injection on *P. berghei* infection.

Fig. S11. Effect of hemocyte disruption by bead polystyrene injection and infection on the relative expression of several functional markers.

Fig. S12. Effect of polystyrene bead injection on the intensity of *TEP1* staining on the ookinete surface.

Fig. S13. Effect of epithelial nitration on the percentage of ookinete-invaded cells positive for hemocyte-derived microvesicles (*HdMv*⁺).

Fig. S14. Effect of epithelial nitration on microvesicle release.

Fig. S15. Effect of epithelial nitration on the percentage of ookinete-invaded cells positive for hemocyte-derived microvesicles (*HdMv*⁺) that are also positive for nitrotyrosine staining.

Fig. S16. Top view maximum intensity projection showing the spatial distribution of Sua5.1 cells in direct contact with the surface of a fixed midgut embedded in a collagen matrix.

Fig. S17. Viability of Sua5.1 cells associated with the collagen matrix interphase in the absence of physical contact with nitrated or non-nitrated (control) midguts after 6 hours of cocubation.

Table S1. Quantification of CM-Dil from dissected midguts.

Table S2. Effect of hemocyte disruption by systemic injection of polystyrene beads on the prevalence of TEP1 staining in *Plasmodium* ookinetes.

Table S3. Effect of midgut nitration on microvesicle release.

Table S4. Induction of apoptosis (caspase activity) in Sua5.1 cells in response to contact with a nitrated collagen matrix surface for 3 hours.

Table S5. Induction of apoptosis (loss of cellular integrity) in Sua5.1 cells in response to 6 hours of exposure to a nitrated midgut and control (non-nitrated).

Table S6. List of primers used for gene expression analysis and for dsRNA synthesis.

Movie S1. Example of the response of Sua5.1 cells to contact with a non-nitrated midgut (replicate #1).

Movie S2. Example of the response of Sua5.1 cells to contact with a non-nitrated midgut (replicate #2).

Movie S3. Example of the response of Sua5.1 cells to contact with a nitrated midgut (replicate #1).

Movie S4. Example of the response of Sua5.1 cells to contact with a nitrated midgut (replicate #2).

Movie S5. Example of the response of Sua5.1 cells that are in the same chamber as nitrated midguts but do not come in contact with the midgut surface.

Reference (25, 26)

REFERENCES AND NOTES

- J. F. Hillyer, S. L. Schmidt, B. M. Christensen, Rapid phagocytosis and melanization of bacteria and *Plasmodium* sporozoites by hemocytes of the mosquito *Aedes aegypti*. *J. Parasitol.* **89**, 62–69 (2003).
- J. K. Nayar, J. W. Knight, A. C. Vickery, Intracellular melanization in the mosquito *Anopheles quadrimaculatus* (Diptera: Culicidae) against the filarial nematodes, *Brugia* spp. (Nematoda: Filarioidea). *J. Med. Entomol.* **26**, 159–166 (1989).
- S. Blandin, S.-H. Shiao, L. F. Moita, C. J. Janse, A. P. Waters, F. C. Kafatos, E. A. Levasina, Complement-like protein TEP1 is a determinant of vectorial capacity in the malaria vector *Anopheles gambiae*. *Cell* **116**, 661–670 (2004).
- S. B. Pinto, F. Lombardo, A. C. Koutsos, R. M. Waterhouse, K. McKay, C. An, C. Ramakrishnan, F. C. Kafatos, K. Michel, Discovery of *Plasmodium* modulators by genome-wide analysis of circulating hemocytes in *Anopheles gambiae*. *Proc. Natl. Acad. Sci. U.S.A.* **106**, 21270–21275 (2009).
- J. Rodrigues, F. A. Brayner, L. C. Alves, R. Dixit, C. Barillas-Mury, Hemocyte differentiation mediates innate immune memory in *Anopheles gambiae* mosquitoes. *Science* **329**, 1353–1355 (2010).
- Y. S. Han, J. Thompson, F. C. Kafatos, C. Barillas-Mury, Molecular interactions between *Anopheles stephensi* midgut cells and *Plasmodium berghei*: The time bomb theory of ookinete invasion of mosquitoes. *EMBO J.* **19**, 6030–6040 (2000).
- S. Kumar, L. Gupta, Y. S. Han, C. Barillas-Mury, Inducible peroxidases mediate nitration of *Anopheles* midgut cells undergoing apoptosis in response to *Plasmodium* invasion. *J. Biol. Chem.* **279**, 53475–53482 (2004).
- G. de Almeida Oliveira, J. Lieberman, C. Barillas-Mury, Epithelial nitration by a peroxidase/NOX5 system mediates mosquito antiplasmodial immunity. *Science* **335**, 856–859 (2012).
- M. Povelones, L. Bhagavatula, H. Yassine, L. A. Tan, L. M. Upton, M. A. Osta, G. K. Christophides, The CLIP-domain serine protease homolog SPCLIP1 regulates complement recruitment to microbial surfaces in the malaria mosquito *Anopheles gambiae*. *PLoS Pathog.* **9**, e1003623 (2013).
- R. C. Smith, C. Barillas-Mury, M. Jacobs-Lorena, Hemocyte differentiation mediates the mosquito late-phase immune response against *Plasmodium* in *Anopheles gambiae*. *Proc. Natl. Acad. Sci. U.S.A.* **112**, E3412–E3420 (2015).
- J. G. King, J. F. Hillyer, Infection-induced interaction between the mosquito circulatory and immune systems. *PLoS Pathog.* **8**, e1003058 (2012).
- P. D. Robbins, A. E. Morelli, Regulation of immune responses by extracellular vesicles. *Nat. Rev. Immunol.* **14**, 195–208 (2014).
- J. L. Ramirez, G. de Almeida Oliveira, E. Calvo, J. Dalli, R. A. Colas, C. N. Serhan, J. M. Ribeiro, C. Barillas-Mury, A mosquito lipoxin/lipocalin complex mediates innate immune priming in *Anopheles gambiae*. *Nat. Commun.* **6**, 7403 (2015).
- C. Frolet, M. Thoma, S. Blandin, J. A. Hoffmann, E. A. Levasina, Boosting NF- κ B-dependent basal immunity of *Anopheles gambiae* aborts development of *Plasmodium berghei*. *Immunity* **25**, 677–685 (2006).
- J. L. Ramirez, L. S. Garver, F. A. Brayner, L. C. Alves, J. Rodrigues, A. Molina-Cruz, C. Barillas-Mury, The role of hemocytes in *Anopheles gambiae* antiplasmodial immunity. *J. Innate Immun.* **6**, 119–128 (2014).
- M. Elrod-Erickson, S. Mishra, D. Schneider, Interactions between the cellular and humoral immune responses in *Drosophila*. *Curr. Biol.* **10**, 781–784 (2000).
- S. Kumar, A. Molina-Cruz, L. Gupta, J. Rodrigues, C. Barillas-Mury, A peroxidase/dual oxidase system modulates midgut epithelial immunity in *Anopheles gambiae*. *Science* **327**, 1644–1648 (2010).
- H. M. Müller, G. Dimopoulos, C. Blass, F. C. Kafatos, A hemocyte-like cell line established from the malaria vector *Anopheles gambiae* expresses six prophenoloxidase genes. *J. Biol. Chem.* **274**, 11727–11735 (1999).
- B. Franke-Fayard, H. Trueman, J. Ramesar, J. Mendoza, M. van der Keur, R. van der Linden, R. E. Sinden, A. P. Waters, C. J. Janse, A *Plasmodium berghei* reference line that constitutively expresses GFP at a high level throughout the complete life cycle. *Mol. Biochem. Parasitol.* **137**, 23–33 (2004).
- O. Billker, M. K. Shaw, G. Margos, R. E. Sinden, The roles of temperature, pH and mosquito factors as triggers of male and female gametogenesis of *Plasmodium berghei* in vitro. *Parasitology* **115**, 1–7 (1997).
- J. C. Castillo, A. E. Robertson, M. R. Strand, Characterization of hemocytes from the mosquitoes *Anopheles gambiae* and *Aedes aegypti*. *Insect Biochem. Mol. Biol.* **36**, 891–903 (2006).
- E. G. Blish, W. J. Dyer, A rapid method of total lipid extraction and purification. *Can. J. Biochem. Physiol.* **37**, 911–917 (1959).
- K. J. Livak, T. D. Schmittgen, Analysis of relative gene expression data using real-time quantitative PCR and the 2^{- $\Delta\Delta$ CT} method. *Methods* **25**, 402–408 (2001).
- M. Povelones, R. M. Waterhouse, F. C. Kafatos, G. K. Christophides, Leucine-rich repeat protein complex activates mosquito complement in defense against *Plasmodium* parasites. *Science* **324**, 258–261 (2009).
- R. C. Smith, A. G. Eappen, A. J. Radtke, M. Jacobs-Lorena, Regulation of anti-*Plasmodium* immunity by a *LITAF*-like transcription factor in the malaria vector *Anopheles gambiae*. *PLoS Pathog.* **8**, e1002965 (2012).
- U. N. Ramphul, L. S. Garver, A. Molina-Cruz, G. E. Canepa, C. Barillas-Mury, *Plasmodium falciparum* evades mosquito immunity by disrupting JNK-mediated apoptosis of invaded midgut cells. *Proc. Natl. Acad. Sci. U.S.A.* **112**, 1273–1280 (2015).

Acknowledgments: We thank S. Ganesan and the Biological Imaging facility at the National Institute of Allergy and Infectious Diseases (NIAID)/NIH for providing training and assistance in confocal microscopy; M. Povelones (University of Pennsylvania) for providing the TEP1 antibody; J. Ribeiro, A. Molina-Cruz, and J. Valenzuela for comments and insight; and A. Laughinghouse and K. Lee for insectary support. **Funding:** This work was supported by the Intramural Research Program of the Division of Intramural Research Z01 AI000947, NIAID, NIH. A.B.B.F. was supported by Ph.D. fellowships from the Brazilian Science Without Borders program from the Conselho Nacional de Desenvolvimento Tecnológico and the Instituto Nacional de Ciencia e Tecnologia em Entomologia Molecular. **Author contributions:** J.C.C. and C.B.-M. did the conceptualization and experimental design; J.C.C. performed in vivo experiments and data analysis; A.B.B.F. and N.T. designed, performed, and analyzed nitration experiments with cultured cells and processed videos and data; J.C.C. and C.B.-M. wrote the manuscript; and C.B.-M. supervised the study. **Competing interests:** The authors declare that they have no competing interests.

Submitted 4 October 2016
Accepted 14 December 2016
Published 20 January 2017
10.1126/sciimmunol.aal1505

Citation: J. C. Castillo, A. B. B. Ferreira, N. Trisnadi, C. Barillas-Mury, Activation of mosquito complement antiplasmodial response requires cellular immunity. *Sci. Immunol.* **2**, eal1505 (2017).

Activation of mosquito complement antiplasmodial response requires cellular immunity

Julio César Castillo, Ana Beatriz Barletta Ferreira, Nathanie Trisnadi and Carolina Barillas-Mury

Sci. Immunol. 2, (2017)

doi: 10.1126/sciimmunol.aal1505

Editor's Summary More than a vector Mosquitoes--the bane of lovers of the outdoors--are also carriers of serious diseases, including malaria, dengue, and Zika virus. Why does the mosquito itself not succumb to infection? Castillo et al. now report that the mosquito immune response to Plasmodium requires cellular immunity. They found that midgut nitration that results from Plasmodium infection in mosquitoes triggered the release of hemocyte-derived microvesicles and that these microvesicles were necessary for the activation of the mosquito complement-like system, which limits Plasmodium infection. Nitration-mediated hemocyte activation may parallel innate immune response to tissue damage in other organisms and shows a clear role for cellular immunity in the mosquito response to infection.

You might find this additional info useful...

This article cites 26 articles, 11 of which you can access for free at:

<http://immunology.sciencemag.org/content/2/7/eaal1505.full#BIBL>

Updated information and services including high resolution figures, can be found at:

<http://immunology.sciencemag.org/content/2/7/eaal1505.full>

Additional material and information about **Science Immunology** can be found at:

<http://www.sciencemag.org/journals/immunology/mission-and-scope>

This information is current as of January 31, 2017.

Science Immunology (ISSN 2375-2548) publishes new articles weekly. The journal is published by the American Association for the Advancement of Science (AAAS), 1200 New York Avenue NW, Washington, DC 20005. Copyright 2016 by The American Association for the Advancement of Science; all rights reserved. Science Immunology is a registered trademark of AAAS